Acetate, a metabolic product of *Heligmosomoides polygyrus*, facilitates intestinal epithelial barrier breakdown in a FFAR2-dependent manner

Fabian Schälter [a], Michael Frech [a], Kerstin Dürholz [a], Sébastien Lucas [a], Kerstin Sarter [a], Luc Lebon [b], Julia Esser-von Bieren [b,c], Lalit K. Dubey [b,d], David Voehringer [e], Georg Schett [a], Nicola L. Harris [b,f], Mario M. Zaiss [a,b,*]

[a] *Department of Internal Medicine 3, Rheumatology and Immunology, Friedrich-Alexander-University Erlangen-Nürnberg (FAU) and Universitätsklinikum Erlangen, Erlangen, Germany*
[b] *Global Health Institute, School of Life Sciences, École Polytechnique Fédérale de Lausanne (EPFL), Lausanne CH-1015, Switzerland*
[c] *Center of Allergy and Environment, Technical University of Munich and Helmholtz Zentrum München, Munich, Germany*
[d] *Centre of Microvascular Research, William Harvey Research Institute, Barts and The London School of Medicine and Dentistry, Queen Mary University of London, London EC1M 6BQ, United Kingdom*
[e] *Department of Infection Biology, University Hospital Erlangen and Friedrich-Alexander University Erlangen-Nürnberg (FAU), Erlangen, Germany*
[f] *Department of Immunology, Monash University, Clayton, Victoria, Australia*

ARTICLE INFO

ABSTRACT

Approximately 2 billion people worldwide and a significant part of the domestic livestock are infected with soil-transmitted helminths, of which many establish chronic infections causing substantial economic and welfare burdens. Beside intensive research on helminth-triggered mucosal and systemic immune responses, the local mechanism that enables infective larvae to cross the intestinal epithelial barrier and invade mucosal tissue remains poorly addressed. Here, we show that *Heligmosomoides polygyrus* infective L3s secrete acetate and that acetate potentially facilitates paracellular epithelial tissue invasion by changed epithelial tight junction claudin expression. In vitro, impedance-based real-time epithelial cell line barrier measurements together with ex vivo functional permeability assays in intestinal organoid cultures revealed that acetate decreased intercellular barrier function via the G-protein coupled free fatty acid receptor 2 (FFAR2, GPR43). In vivo validation experiments in FFAR2$^{-/-}$ mice showed lower *H. polygyrus* burdens, whereas oral acetate-treated C57BL/6 wild type mice showed higher burdens. These data suggest that locally secreted acetate – as a metabolic product of the energy metabolism of *H. polygyrus* L3s – provides a significant advantage to the parasite in crossing the intestinal epithelial barrier and invading mucosal tissues. This is the first and a rate-limiting step for helminths to establish chronic infections in their hosts and if modulated could have profound consequences for their life cycle.

© 2022 Australian Society for Parasitology. Published by Elsevier Ltd. All rights reserved.

1. Introduction

Chronic soil-transmitted helminth infections remain an immense global health problem and although not fatal, they are associated with high morbidity rates, caused by chronic infections often leading to anemia and malnourishment in both humans and livestock (de Silva et al., 2003). Here, we used *Heligmosomoides polygyrus* as a natural mouse helminth model organism, to explore general mechanisms of initial host tissue invasion before the well-studied immune evasion mechanisms come into play (Behnke et al., 2009; Harris and Gause, 2011; Reynolds et al., 2012; Harris et al., 2014). Of note, helminth infections are different from other pathogen encounters as a simple measure of their size that is significantly larger than bacteria, fungi and viruses or classical host immune cells. Typically, helminths elicit a type 2 dominated immune response (Anthony et al., 2007). However, intestinal epithelial cells are obviously the first host contact cells of infective larvae that need to be tackled in order to establish successful chronic infections (Wojciechowski et al., 2009). So far intestinal epithelial cells were functionally considered to sense parasite-derived and damage-associated molecules and secreted alarmin type cytokines that in turn initiate systemic type 2 immune responses whereas local mechanisms facilitating *H. polygyrus* bar-

* Corresponding author at: Department of Internal Medicine 3, Rheumatology and Immunology, Friedrich-Alexander-University Erlangen-Nürnberg (FAU) and Universitätsklinikum Erlangen, Universitätsstrasse 25A, 91054 Erlangen, Germany.
E-mail address: mario.zaiss@uk-erlangen.de (M.M. Zaiss).

rier penetration remain incompletely understood (Sina et al., 2009; Wojciechowski et al., 2009; McKay et al., 2017).

Here we investigated a novel mechanism that facilitates the first critical step of the *H. polygyrus* life cycle – namely host tissue invasion. *Heligmosomoides polygyrus* infection was previously shown not to cause intestinal epithelial cells (IEC) damage (Sutton et al., 2008), suggesting that *H. polygyrus* enters the submucosa paracellularly. One of the molecules that we recently identified among the excretory-secretory products (ESP) of adult *H. polygyrus* worms is acetate, the anion of the acetic acid and a short-chain fatty acid (SCFA) (Zaiss et al., 2015). Acetate was also detected within the ESP of other helminthic parasites (Tielens et al., 2010). Moreover, as acetate was shown to elicit various effects on epithelial and immune cells, we anticipated a potential impact on IECs during the tissue invasion phase of *H. polygyrus* (Thorburn et al., 2015).

By applying state of the art barrier assays, we describe a functional role for acetate in breaching the intestinal epithelial barrier. Our experiments delineate free fatty acid receptor (FFAR) expression on the IEC as critical for this effect as shown by FFAR loss-of-function intestinal-organoid assays. In particular, we linked these general mechanistic in vitro observations to the physiologically relevant issue of host tissue penetration by helminths. Our data suggest that acetate facilitates tissue invasion of infective helminth larvae through IEC tight junction degradation as a first critical step in their life cycle.

2. Materials and methods

2.1. Mice, parasites and treatments

C57BL/6J and FFAR2$^{-/-}$ mice were bred and maintained under specific pathogen-free conditions at Ecole Polytechnique Fédérale de Lausanne (EPFL) or Centre Hospitalier Universitaire Vaudois (CHUV) at Epalinges, Switzerland. All mice were co-housed for 2 weeks prior to parasite infection and/or treatments. Where indicated, mice were infected with 200 *H. polygyrus* L3s. For acetate supplementation mice were fed with 150 mM acetate in the drinking water. Adult worm burdens and granuloma numbers were determined by manual counting using a dissecting microscope.

2.2. Flow cytometry

Spleens and lymph nodes were crushed on 40 μm gauze and filtered through 40 μm gauze (BD Biosciences, Franklin Lakes, NJ, USA). Single-cell suspensions were then stained for flow cytometry with the following antibodies: CD3 FITC (clone HIT3a), CD4 Pacific blue (clone GK1.5), IL-4 PE (clone 11B11), IL-13 APC (clone SS12B), CD45 Brilliant Violet 650 (clone HI30). Fluorescence was detected using a BD LSR II (BD Biosciences) and data was analysed using FlowJo Software (version 10.8.1). Representative gating strategy is shown in Supplementary Fig. S1.

2.3. Acetate measurement

For short-chain fatty acid (SCFA) analysis, the samples were derivatized prior to gas chromatography-mass spectrometry (GC–MS) analyses using N-tert-Butyldimethylsilyl-N-methyltrifluoroa cetamide (MTBSTFA) + 1% tert-Butyldimethylsilyl trifluoromethanesulfonate (TBDMCS) as a silylation reagent (Thermo Scientific, Waltham, MA, USA). Samples 60 μl; in duplicate) were incubated with 20 μl of reagent for 1 h at room temperature. For the calibration curve, 60 μl of the acetate standards were dissolved in acetonitrile (Thermofisher) and derivatized by addition of 20 μl of reagent for 1 h at room temperature. All samples were run on a

CP-3800 Gas Chromatograph coupled to a 1200 L Quadrupole MS/MS (Varian, Palo Alto, CA, USA) using a FactorFour VF-50 ms, 30 m × 0.25 mm × 0.25 mm capillary column (Varian). The carrier gas was helium and the column flow was 1 ml/min. The injector, transfer line and MS source were set to 250 °C, 250 °C and 200 °C, respectively. The oven program was as follows: 50 °C initial for 2 min, then 20 °C/min to 150 °C for 5 min, then 30 °C/min to 250 °C for 5 min. Sample (2 μl) was injected and GC–MS analyses performed in duplicates. Full scan mass spectra were recorded in the 50–450 m/z range (1 s/scan). Quantification was done by integration of the extracted ion chromatogram peaks following ion species: m/z 117 and 75 for acetate eluted at 5.2 min.

2.4. Cell isolation and generation of murine intestinal organoids from mouse intestine

Wild type (WT) C57BL/6J mice were sacrificed by cervical dislocation and the small intestine was removed. The intestine was washed with ice-cold PBS and opened longitudinally. The villi were scraped out using a glass coverslip and discarded. The tissue was cut into 2–3 mm pieces, collected in ice-cold PBS and allowed to settle by gravity. After sedimentation the PBS was discarded, fresh ice-cold PBS was added and the sample lightly shaken. This washing procedure was repeated 15–20 times until the supernatant was clear and no intestinal contents were visible. Following washing, the tissue was incubated in crypt isolation buffer (2 mM EDTA in PBS) at 4 °C for 20 min while agitating. After the incubation time the tissue pieces were sedimented by gravity and the supernatant was discarded. Fresh ice-cold PBS was added and the Falcon tube was vigorously shaken to dissociate stem cells from the tissue. Then the supernatant was collected and marked as fraction #1 and screened for intestinal crypts by microscopy. This step was repeated 5–6 times until no crypts were detected in the supernatants. The fractions that were enriched in intestinal crypts were then filtered through a 70 μm cell strainer and centrifuged at 300 *g* for 5 min at 4 °C. The supernatant was discarded and the cell pellet was resuspended in 25 μl/well of Matrigel (Corning, Corning, NY, USA). This suspension was distributed into a 48-well cell culture plate. For polymerisation of the Matrigel, the plate was incubated at 37 °C and 5% CO_2 for 20 min. After polymerization, 300 μl of Intesticult Organoid Growth medium (Stem cell, Vancouver, Canada) were added per well. The organoids were cultured for 7 days and then passaged at least once before they were used for experiments. Medium was changed every 2 days and the intestinal organoids were split once per week (Sato et al., 2009).

2.5. Confocal imaging and permeability assay

For the permeability assay, organoids were cultured in 8-well Ibidi chamber slides for 48 h after splitting prior to imaging, to keep the organoids from budding. For the confocal imaging a Zeiss Spinning Disc confocal microscope was used. First positions of the desired organoids were determined and set for imaging. Then 1 mM lucifer yellow (LY) was added to each well of the chamber slide. The organoids were imaged for 100 min at intervals of 5 min. To exclude organoids that can't be permeabilized, 1 mM EGTA was added and organoids were imaged for another 20 min at 5 min intervals. For each time point LY fluorescence inside and outside the organoid was quantified using ImageJ (version 1.53p). Organoids that did not become permeable were excluded from the analysis (Bardenbacher et al., 2019).

2.6. Preparation of fecal supernatants

Intestinal stool samples were obtained from *H. polygyrus*-infected and non-infected C57BL/6J mice after 3 weeks of infection.

The stool samples were suspended in PBS at 10% (wt/vol), homogenised and centrifuged at 4000 *g* for 10 min at 4 °C. Solid contents were discarded and the supernatants were passed through a 1.2 µm membrane filter (Tajik et al., 2020).

2.7. Generation and collection of H. polygyrus ESPs (HESPs)

For the generation of *H. polygyrus* ESPs (HESPs), helminths were washed extensively in sterile PBS supplemented with penicillin and streptomycin (Gibco, Thermo Fisher), then incubated for 1 h in RPMI (Gibco, Thermo Fisher) supplemented with penicillin and streptomycin, and cultured in RPMI plus antibiotics (penicillin, streptomycin, and gentamicin; Sigma–Aldrich, St. Louis, MO, USA) and 1% glucose (Sigma–Aldrich). The supernatant was collected every 2 days for a period of 2 weeks, followed by sterile filtration and concentration of the supernatant by centrifugation through a 10,000 molecular weight cut-off (MWCO) cellulose membrane (Centriprep; Millipore). Lipopolysaccharide (LPS) contamination was removed from HESPs using an EndoTrap Blue LPS-binding affinity column (Hyglos GmbH, Bernried, Germany). The concentration of residual endotoxin was determined using the Limulus Assay, which has a sensitivity of 0.06 endotoxin units/ml (6 pg/ml) (Lonza, Bend, USA). The final preparation used for this study contained 31 pg/ml of LPS in the pyrogen-free HESPs (P.HESPs) versus 643 pg/ml in the non-purified HESPs (HESPs). The same batch of pyrogen-free HESP was used for all the experiments shown in this study.

2.8. Wholemount immunofluorescence staining of intestinal organoids

For immunostaining, organoids were cultured in 8-well Ibidi chamber slides and treated for 24 h with acetate. After treatment the organoids were washed three times with ice-cold PBS and afterwards fixed by incubation with 4% paraformaldehyde for 30 min at room temperature. After fixation organoids were permeabilized in 0.5% Triton-X100 diluted in Tris-buffered saline for 30 min at ambient temperature. Rabbit anti claudin-7 primary antibody (Invitrogen, Waltham, MA, USA) were incubated overnight at 4 °C. After washing, organoids were incubated with donkey anti-rabbit secondary antibody (Invitrogen) for 7 h at ambient temperature. The nuclei were counterstained with DAPI containing mounting medium. Imaging was performed with a Zeiss Spinning Disc Axio Z1 live cell observer (Bardenbacher et al., 2019).

2.9. Quantification of spatial disorganisation

Tubular structures in the images were first enhanced using the Fiji tubeness filter with a smoothing factor of 1.2 pixels. The filtered images were binarized using a manually adjusted global threshold. The Fiji local thickness plugin was then applied to assign a local thickness value to each pixel. Pixels with a thickness value below 6 pixels were found to belong to small bubbles, while pixels with a local thickness above 6 belonged to cell bodies. Finally, the ratio of the number of pixels belonging to bubbles and the number of pixels belonging to cell bodies was calculated for each image.

2.10. Propidiumiodide/annexin V cell viability assay

To detect cell death, murine intestinal organoids were recovered from;three-dimensional (3D) culture using Cell Recovery Solution (Corning). Afterwards organoids were incubated in Trypsin-EDTA (0.05%) (Fisher scientific, Waltham, MA, USA) at 37 °C for 10 min to dissociate them into a single cell solution. Single cells were stained with 1 µg of annexinV-FITC and 1 µg of propidiumiodide per 1×10^6 cells for 10 min at ambient temperature, protected from light. Fluorescence was detected using a Cytoflex S

flow cytometer (Beckman Coulter, Brea, CA, USA) and analysed using Kaluza analysis software (Beckman Coulter). As a positive control, cells were radiated with UV light (160 mJ/cm^{2}min) for 5 min to induce apoptosis.

2.11. Trans-well assay

Caco-2 cells (5×10^5/well) were seeded in 24-well trans-well inserts with a pore size of 0.4 µm (Greiner Bio-One, Frickenhausen, Germany). Trans-epithelial electrical resistance was measured daily until a plateau was reached, to determine cell confluency. After confluency was reached, FITC-dextran with a size of 3–5 kDa (Sigma-Aldrich) was added to the inserts for 4 h. Afterwards, culture media from the well plates were analysed using a fluorescence 96-well plate reader Infinite 200 Pro (Tecan, Männedorf, Switzerland). The excitation and emission wavelengths were 490 and 530, respectively.

2.12. Immunofluorescence staining

Small intestine of infected mice was fixed in 4% formalin for 4 h. Serial paraffin sections (2 µm) were deparaffinized and rehydrated in Xylol (ROTI Histol, Carl Roth, Karlsruhe, Germany) and decreasing concentrations of isopropanol. Antigen retrieval was performed for 15 min at 90 °C in citrate buffer. The slides were washed, then blocked in 5% milk for 30 min and then stained with rabbit anti-mouse acetylated-lysine primary antibody (Merck, Darmstadt, Germany) overnight at 4 °C. After washing, the slides were stained with Alexa Fluor 647 donkey anti-rabbit secondary antibody (Invitrogen). Slides were then mounted with Fluoroshield mounting medium (Abcam, Cambridge, UK) and analysed using a Leica SP8 confocal microscope.

2.13. Maestro Z impedance measurements

Prior to cell plating, 100 µL of DMEM/2% FBS were added to each well of CytoView-Z 96-well electrode plates (Axion Biosystems, Atlanta, GA, USA). CytoView-Z plates ware then docked into the Maestro Z instrument to measure the impedance electrode baseline. Caco-2 cells (~16,000 cells/well) were then added in the CytoView-Z plates and left at room temperature for 1 h to ensure even coverage of the well. Plates containing Caco-2 cells were then docked into the Maestro Z for up to 96 h at 37 °C/5% CO$_2$ to allow the cells to attach and the monolayer to reach confluency, as measured by resistance, a component of impedance. The Maestro Z was used to monitor the resistance of the monolayer as it formed, very similar to transepithelial electrical resistance (TEER). In this study, resistance was measured at 41.5 kHz and 1 kHz, which reflects cell coverage over the electrode and strength of the barrier formed by the cell monolayer, respectively. For acetate treatments, a half media change was performed 3 h prior to treatment and then 25 µL of pre-warmed DMEM/2% FBS were added with 0.5 mM or 10 mM acetate. Resistance measurements were continuously recorded for 48–72 h post-treatment at 37 °C/5% CO$_2$ in a humidified environment in the Maestro Z instrument. All plates contained media only, vehicle and acetate-treated samples. Raw resistance values for each well containing acetate were normalised to vehicle and to the value at 10 min prior to acetate treatment. Data analyses were performed in Axis Z software (Axion Biosystems, Atlanta, GA, USA) (Benson et al., 2013).

3. Results

3.1. Acetate supplementation increases worm burden in H. polygyrus-infected mice

In line with our previous report on adult *H. polygyrus* worms (Zaiss et al., 2015), GC–MS analysis of L3 culture supernatants showed increased acetate concentrations (Fig. 1A). As secreted acetate was shown to predominantly drive lysine acetylation (Daïen et al., 2021), we visualised acetate secretion by *H. polygyrus* larvae in vivo by histological analysis of acetylated lysine. Indeed, we found clear positive signals specifically in IECs and lamina propria cells that had been in contact with *H. polygyrus* larvae during tissue invasion (Fig. 1B). Further, to investigate functional consequences of *H. polygyrus*-secreted acetate for *H. polygyrus* infectivity, C57BL/6 WT mice were orally supplemented with 150 mM sodium-acetate in drinking water starting at 0 days p.i. with 200 L3s by oral gavage till 13 days p.i. Following our previous publications (Zaiss et al., 2015; Lucas et al., 2018; Azizov et al., 2020), we defined supplementation of 150 mM sodium acetate in the drinking water as sufficient to increase serum acetate concentrations comparable to the *H. polygyrus*-mediated acetate increase.

Acetate-supplemented WT mice already showed higher worm burdens at 13 days p.i. (Fig. 1C). FFAR2 and FFAR3 (previously GPR41) were shown to be activated by different SCFA (Brown et al., 2003; Brown et al., 2005), whereas acetate was most selective for FFAR2 (Le Poul et al., 2003). While FFAR3$^{-/-}$ mice were reported to exhibit an unchanged host defense (Zaiss et al., 2015), FFAR2$^{-/-}$ mice showed significantly reduced *H. polygyrus* worm burdens as early as 13 days p.i. (Fig. 1C). Acetate was shown to elicit various systemic immunomodulatory effects (Nilsson et al., 2003; Sina et al., 2009; Qiu et al., 2019; Kim, 2021; Yap et al., 2021) and helminth infections robustly initiated type 2 immune responses (Lloyd and Snelgrove, 2018; Moyat et al., 2019). Therefore, we analysed the gut draining mesenteric lymph nodes (mLN) and the spleen. Flow cytometry analyses at 13 days p.i. revealed increased IL-13, but unchanged IL-4, positive CD4 T cells in the spleen (Fig. 1D, E) and IL-13 positive and IL-4 positive CD4 cells in the mLN (Fig. 1F,G) of *H. polygyrus*-infected mice following acetate supplementation. In summary, oral acetate supplementation promoted *H. polygyrus* infectivity whereas loss of the high affinity acetate receptor FFAR2 strongly blunted *H. polygyrus* infectivity. Given the very early changes in *H. polygyrus* worm numbers at 13 days p.i., we next
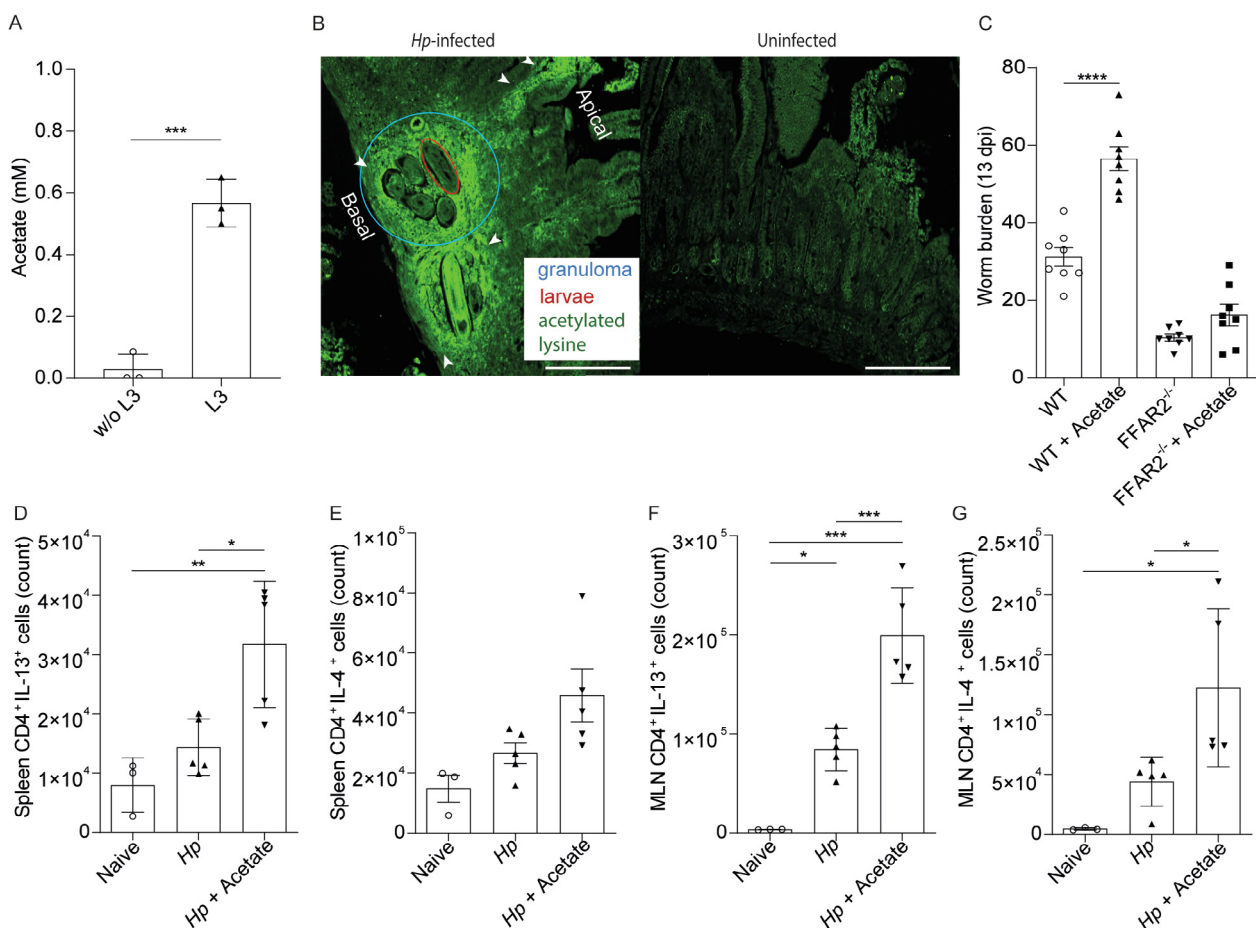
Fig. 1. Effects of acetate during *Heligmosomoides polygyrus* infection in mice. (A) Acetate levels of L3 culture supernatants and controls without larvae (w/o L3) in mmol/l ($n = 3$). Values were compared using an unpaired *t*-test. ***$P < 0.001$. (B) Immunofluorescence staining with anti-acetylated lysine antibody of *H. polygyrus*-infected mouse intestine histological slides (13 days p.i.) with *H. polygyrus* larvae inside the submucosa of the intestine and uninfected mouse intestine as a staining control (scale bar: 200 µm). (C) Worm count at 13 days p.i. (dpi) of *H. polygyrus*-infected wildtype and free fatty acid receptor 2 knockout (FFAR2$^{-/-}$) mice with and without acetate ($n = 5$). Values were compared using one-way ANOVA. ****$P < 0.0001$. (D) IL-13-positive cells in the spleen of naive mice and *H. polygyrus*-infected mice with and without acetate treatment ($n = 3$–5). Values were compared with one-way ANOVA. *$P < 0.05$, **$P < 0.01$. (E) IL-4-positive cells in the spleen of naive mice and *H. polygyrus*-infected mice with and without acetate treatment ($n = 3$–5). Values were compared using one-way ANOVA. (F) IL-13-positive cells in the mesenteric lymph node of naive mice and *H. polygyrus*-infected mice with and without acetate ($n = 3$–5). Values were compared using one-way ANOVA. * $P < 0.05$, *** $P < 0.001$. (G) IL-4-positive cells in the mesenteric lymph node of naive mice and *H. polygyrus*-infected mice with and without acetate treatment ($n = 3$–5). Values were compared using one-way ANOVA. * $P < 0.05$.

investigated potential initial effects of acetate on non-lymphoid cells.

3.2. Acetate drives epithelial barrier breach in intestinal organoids

As *H. polygyrus* infections were shown to leave the intestinal epithelium layer during tissue invasion intact (Sutton et al., 2008) we explored the direct effect of acetate on epithelial barrier permeability in intestinal organoids. Stem cell-derived organoids, compared with spheroids or 2D cell layers, have an in-vivo-like cell composition, and consequently represent a superior system to test effects of effector molecules on the epithelial barrier.

Functional, time-resolved barrier integrity assays of intestinal organoids were described previously (Bardenbacher et al., 2019) and applied to our experiments. As acetate was shown to be secreted by adult *H. polygyrus* (Zaiss et al., 2015), we first stimulated intestinal organoids with HESPs, or live *H. polygyrus* L3s, and analysed intestinal barrier integrity using confocal spinning disc live cell microscopy at 5 min intervals for a period of 70 min. Therefore, LY fluorochrome was added to the intestinal organoid cell cultures to evaluate the intact functional barrier integrity. This resulted in exclusion of LY in the organoid lumen while intraluminal accumulation of LY over time indicated a breach in barrier integrity. In each experimental setup the final addition of EGTA caused an non-specific breakdown of intestinal barrier integrity by sequestering essential tight junction cofactors and was used as a positive control at the end of the experiment to demonstrate the ability of the individually analysed organoids to take up LY intra-luminally (Bardenbacher et al., 2019). When stimulated with HESPs or co-cultured with L3s, intestinal organoids showed increased permeability compared with PBS-treated control organoids as shown by a significantly higher inside/outside fluorescence ratio (Fig. 2A). Interestingly, 20–50 mM acetate treatment – our identified effector molecule secreted by *H. polygyrus* ((Zaiss et al., 2015 and Fig. 1A) – showed similar effects on organoid permeability as shown for HESPs and L3s (Fig. 2B). A physiological mixed combination of the most relevant SCFA (60% acetate, 20% propionate and 20% butyrate) revealed that only acetate increased barrier permeability as opposed to just propionate and butyrate alone, and the physiological SCFA mix showed values in between the single treatments (Supplementary Fig. S2A). Further, additional results from 2D Caco2 monolayers using larger 4 kDa FITC-dextran molecules confirmed this finding for larger molecules (Supplementary Fig. S2B). To exclude treatment-induced apoptosis or necrosis in IECs as an underlying and unifying mechanism of the adverse effects of acetate, PI/AnnexinV-FITC staining and whole-mount immunofluorescence-activated caspase-3 staining were conducted, which repeatedly showed unchanged viability (Fig. 2C, D). Moreover, no macroscopic morphological changes were visible following acetate stimulation with relevant concentrations (Fig. 2E). To further demonstrate the effect of acetate on barrier permeability in a human system, we applied TEER measurements in the human epithelial cell line Caco-2. Non-invasive, continuous cell monitoring in a controlled environmental chamber allowed electrical resistance measurements over time in a 96-well format using the Axion Maestro Z system. In this setting, an already low acetate concentration of 0.5 mM resulted in significantly increased Caco-2 permeability (Fig. 2F, G).

To address additional LPS-derived effects on barrier permeability (Feng et al., 2018), in combination with acetate, intestinal organoids were stimulated with 10 μg/ml of LPS. The addition of 0.5 mM acetate further increased LPS-induced permeability (Fig. 2H), suggesting that acetate can increase intestinal permeability under inflammatory conditions.

3.3. Loss of FFAR2 prevents acetate-induced and L3-induced barrier breach

SCFA can be absorbed by passive diffusion or be transported into the cell by substrate transporters to induce multiple effector functions (den Besten et al., 2013; Lu et al., 2013; Sivaprakasam et al., 2016; Parada Venegas et al., 2019a). SCFA also signal through the metabolite-sensing G protein-coupled receptor FFAR, with acetate showing the highest binding affinity for FFAR2. In contrast to our results using WT (Fig. 2), FFAR2$^{-/-}$ organoids were resistant to 50 mM acetate and HESP treatment, and preserved intact barrier integrity (Fig. 3A, B). However, a tendency towards stronger permeability remained following HESP stimulation in FFAR2$^{-/-}$ organoids (Fig. 3A), which could be attributed to other active components in HESPs (Johnston et al., 2015; White et al., 2020). We previously showed that *H. polygyrus* increases SCFA levels at 25 days p.i., with the highest concentrations of acetate in the small intestinal contents (Zaiss et al., 2015) of infected mice. Therefore, in a more physiological approach we further investigated if fecal supernatants (FSN) – as recently described (Tajik et al., 2020) – derived from intestinal content samples of naive (FSN-naive) versus *H. polygyrus*-infected (FSN-*Hp*) mice maintain or interrupt the barrier integrity, respectively. Here we collected FSN after 3 weeks of *H. polygyrus* infection, because acetate levels were not significantly increased in intestinal contents at 13 days p.i. We suggest that L3s increase acetate locally at their site of tissue invasion, but do not increase the overall intestinal acetate concentration significantly at this stage due to low worm numbers. In both WT (Fig. 3C) and FFAR2$^{-/-}$ (Fig. 3D) organoids, FSN-naive did not change the barrier permeability as shown by non-elevated LY fluorescence inside/outside ratios. Strikingly, the FSN-*Hp* treatment increased the permeability only in WT organoids, whereas no permeability modulating effects were observed in FFAR2$^{-/-}$ organoids (Fig. 3C, D). Further, results following lipid removal of FSN derived from *H. polygyrus*-infected WT mice (Supplementary Fig. S2C, D) suggests that the non-lipid compartment carries most effector molecules responsible for increased barrier permeability in WT organoids (Supplementary Fig. S2C). However this non-lipid compartment is ineffective in increasing barrier permeability in FFAR2−/− organoids (Supplementary Fig. S2D). As acetate dissolves well in water, this dataset further supports our findings of the importance of FFAR2 receptor engagement. For co-incubation of organoids with L3s, a similar trend was seen (Fig. 3E). This supports our hypothesis that intestinal barrier breach of L3s is at least partially mediated by secreted acetate and that higher intestinal acetate levels are beneficial for *H. polygyrus.* Of note, no macroscopic morphological changes were induced by naïve or FSN-*Hp* during the uptake assay (Fig. 3B). This supports our hypothesis that the increased acetate levels in FSN-*Hp* elicits its barrier permeabilizing effect via binding to FFAR2 on IECs rather than by inducing apoptosis or dissociation of the epithelial cells within the organoids.

3.4. Acetate drives Claudin-7 subcellular localization

The regulation of immune cell function by SCFA is manifold and was shown to also impact the intestinal barrier permeability by modulating tight junction (TJ) proteins in IECs (Ohata et al., 2005; Elamin et al., 2013; D'Souza et al., 2017; Feng et al., 2018). Claudins are the major TJ proteins which are critical for maintaining intestinal barrier function (Angelow et al., 2008; Fasano, 2012; Landy et al., 2016). Other than ZO-1 mRNA expression, occludin and typical TJ claudin mRNA expression remained unchanged (Fig. S2E). However, we observed a disrupted localization of claudin-7 in acetate-treated WT organoids whereas FFAR2$^{-/-}$ organoids remained unaffected (Fig. 4A, B, C). In acetate-treated orga-
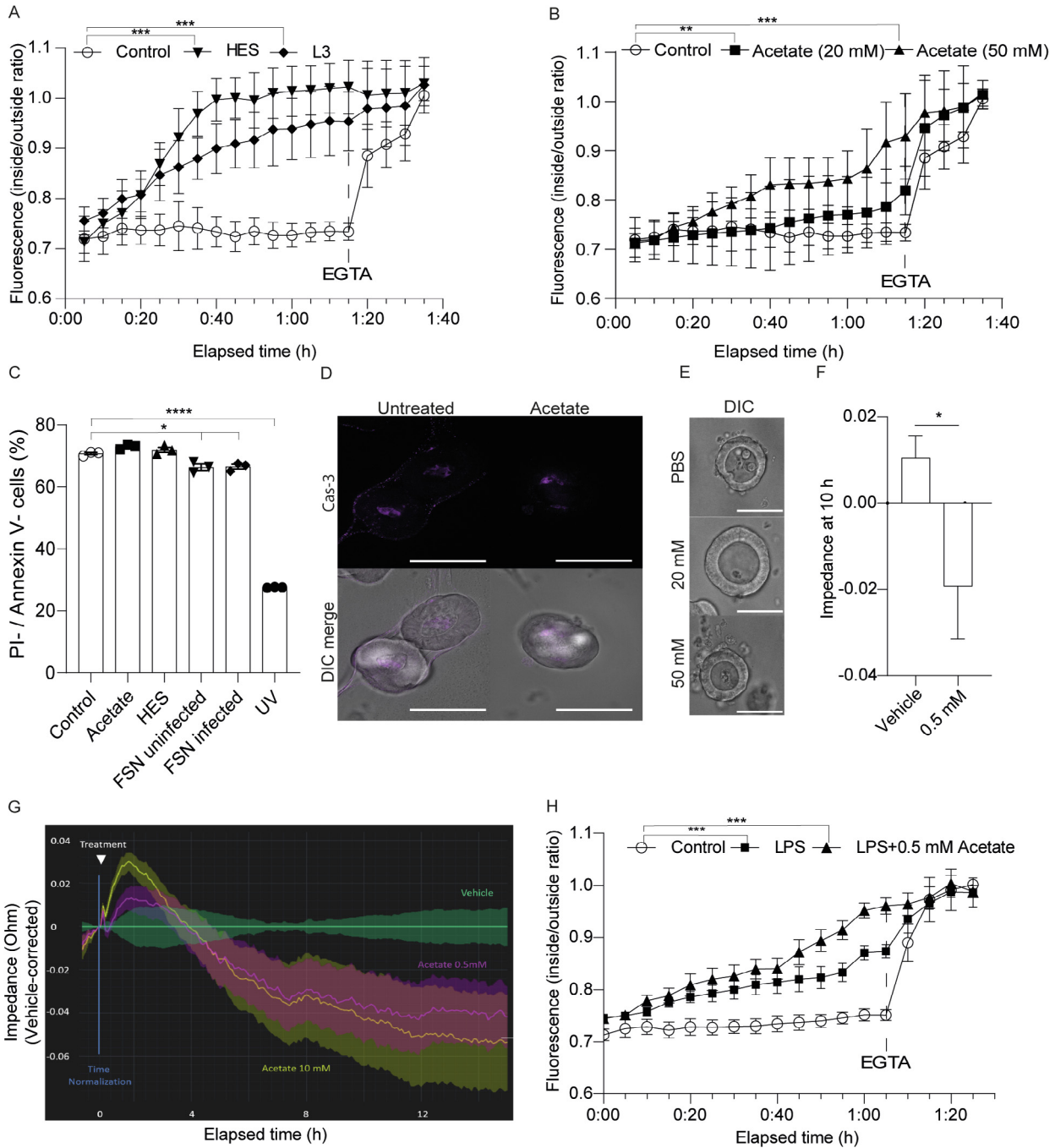
Fig. 2. Acetate mediates barrier permeability in murine intestinal organoids and Caco-2 cells. (A and B) Inside/outside fluorescence ratio of murine intestinal organoids over a time course of 80 min. Afterwards EGTA was added to open up all organoids as positive control. Organoids were stimulated with *Heligmosomoides polygyrus* excretory-secretory products (HES) (diluted 1:500), 200 *Heligmosomoides polygyrus* L3s per well or acetate (*n* = 6–10). Values were compared using two-way ANOVA. **$P < 0.01$, ***$P < 0.001$. (C) Percentage of annexin V-negative, propidiumiodide-negative cells, representing living cells, isolated from organoid culture that were either untreated or treated with acetate, HES or fecal supernatant. UV-radiated cells serve as a positive control (*n* = 3). (D) Paraformaldehyde-fixed organoids were stained with rabbit anti-cleaved-caspase-3 antibody (scale bars: 50 μm). (E) Morphology of treated and untreated organoids in a differential interference contrast picture (scale bars: 50 μm). (F) Quantification of transepithelial electrical resistance at the 10 h timepoint (*n* = 5). Values were compared using one-way ANOVA. *$P < 0.05$. (G) Transepithelial electrical resistance measurement of Caco-2 cell monolayers, stimulated with 0.5 mM or 10 mM, over 12 h at 1 min intervals. (H) Inside/outside fluorescence ratio of murine intestinal organoids over a time course of 85 min. EGTA was added to open up all organoids as a positive control. Organoids were stimulated with 1 ng/ml of lipopolysaccharide alone or lipopolysaccharide together with acetate (*n* = 6–10). Values were compared using two-way ANOVA. ***$P < 0.001$.

noids the claudin-7 staining showed a bubble formation in the intracellular space, similar to the observations of Su et al. (2011) in colonic epithelial cells of *H. polygyrus*-infected mice. A possible explanation for this is that intercellular TJ are destroyed upon acetate stimulation and therefore cells lose cell–cell membrane con-tact. As changes in claudin-7 subcellular localisation have been shown to disrupt epithelial barrier function (Bardenbacher et al., 2019), these results pose a hint that claudin-7 delocalization is involved in an *H. polygyrus* acetate-derived epithelial barrier breach.
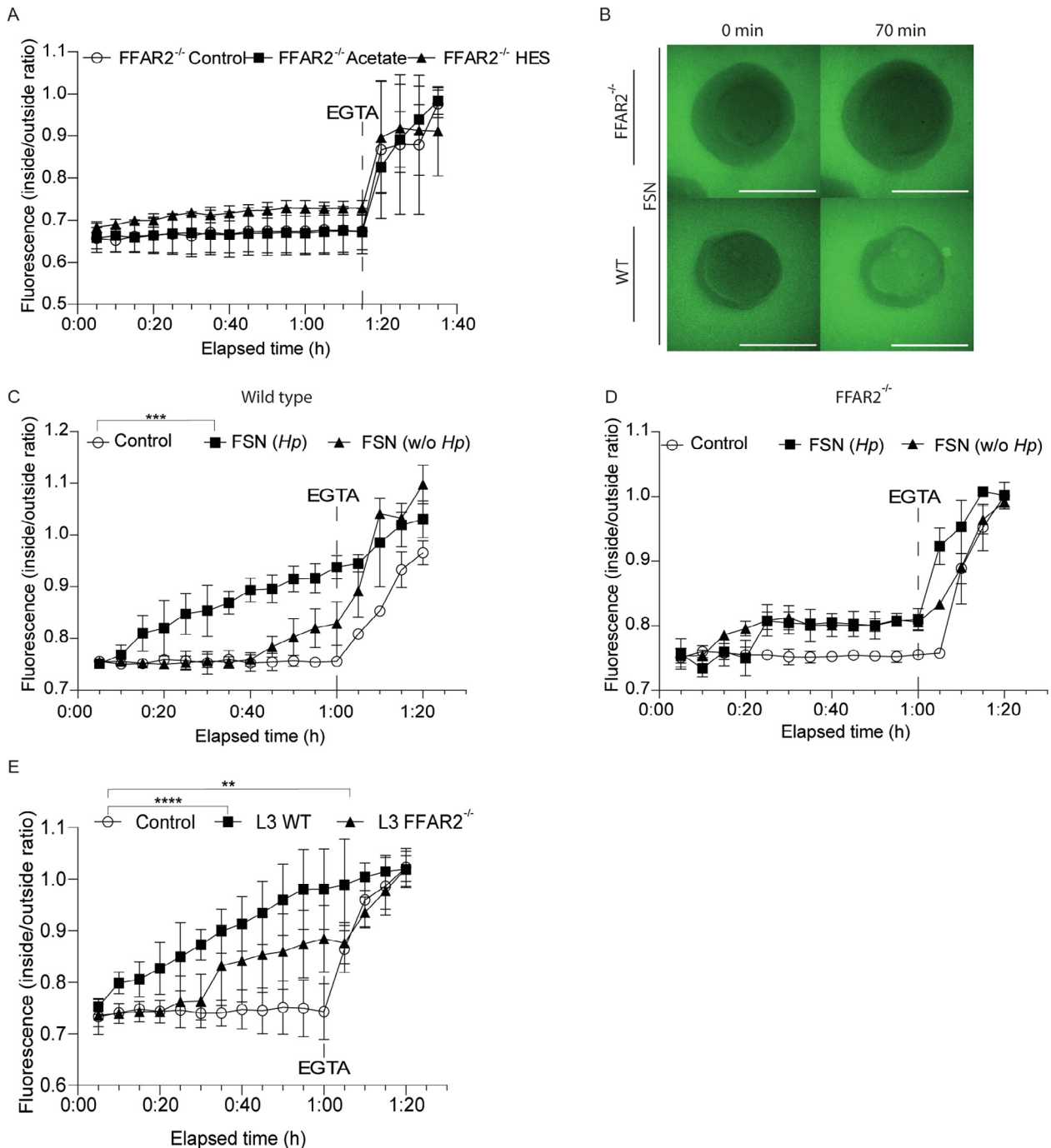
Fig. 3. Murine intestinal organoids of free fatty acid receptor 2 knockout (FFAR2$^{-/-}$) mice are resistant to acetate-induced increased permeability. (A) Inside/outside fluorescence ratio of murine intestinal organoids from FFAR2$^{-/-}$ mice over a time course of 95 min. Organoids were stimulated with *Heligmosomoides polygyrus* excretory-secretory products (HES) or acetate (n = 6–10). Values were compared using two-way ANOVA. Afterwards EGTA was added to open up all organoids as a positive control. (B) Confocal laser fluorescence images of wildtype and FFAR2$^{-/-}$ organoids at 0 min and 70 min within the lucifer-yellow-fluorescence-based uptake assay (scale bars: 50 μm). FSN, fecal supernatant. (C and D) Inside/outside fluorescence ratio of murine intestinal organoids from FFAR2$^{-/-}$ mice or wildtype mice over a time course of 80 min. Afterwards EGTA was added to open up all organoids as a positive control. Organoids were stimulated with fecal supernatant from *Heligmosomoides polygyrus*-infected (*Hp*) or uninfected (w/o *Hp*) mice (n = 6–10). Values were compared using two-way ANOVA. ***P < 0.001. (E) Inside/outside fluorescence ratio of murine intestinal organoids from FFAR2$^{-/-}$ mice or wildtype mice over a time course of 80 min. Afterwards EGTA was added to open up all organoids as a positive control. Organoids were stimulated with 200 *H. polygyrus* L3s per well (P = 6–10). Values were compared using two-way ANOVA. **P < 0.01, ***P < 0.001.

4. Discussion

It has been shown that helminth infections cause an intestinal barrier breach as a consequence of the host's immune response (Su et al., 2011; Wolff et al., 2012; McKay et al., 2017). It is crucial to differentiate between this secondary barrier breach, following the provoked immune response that is beneficial to the host, supporting the expulsion of the invading parasite (Anthony et al., 2007), and the here investigated initial barrier breach, preceding the immune response and benefiting the parasite in its attempt to enter the intestinal tissue (Behnke et al., 2009; Johnston et al., 2015).
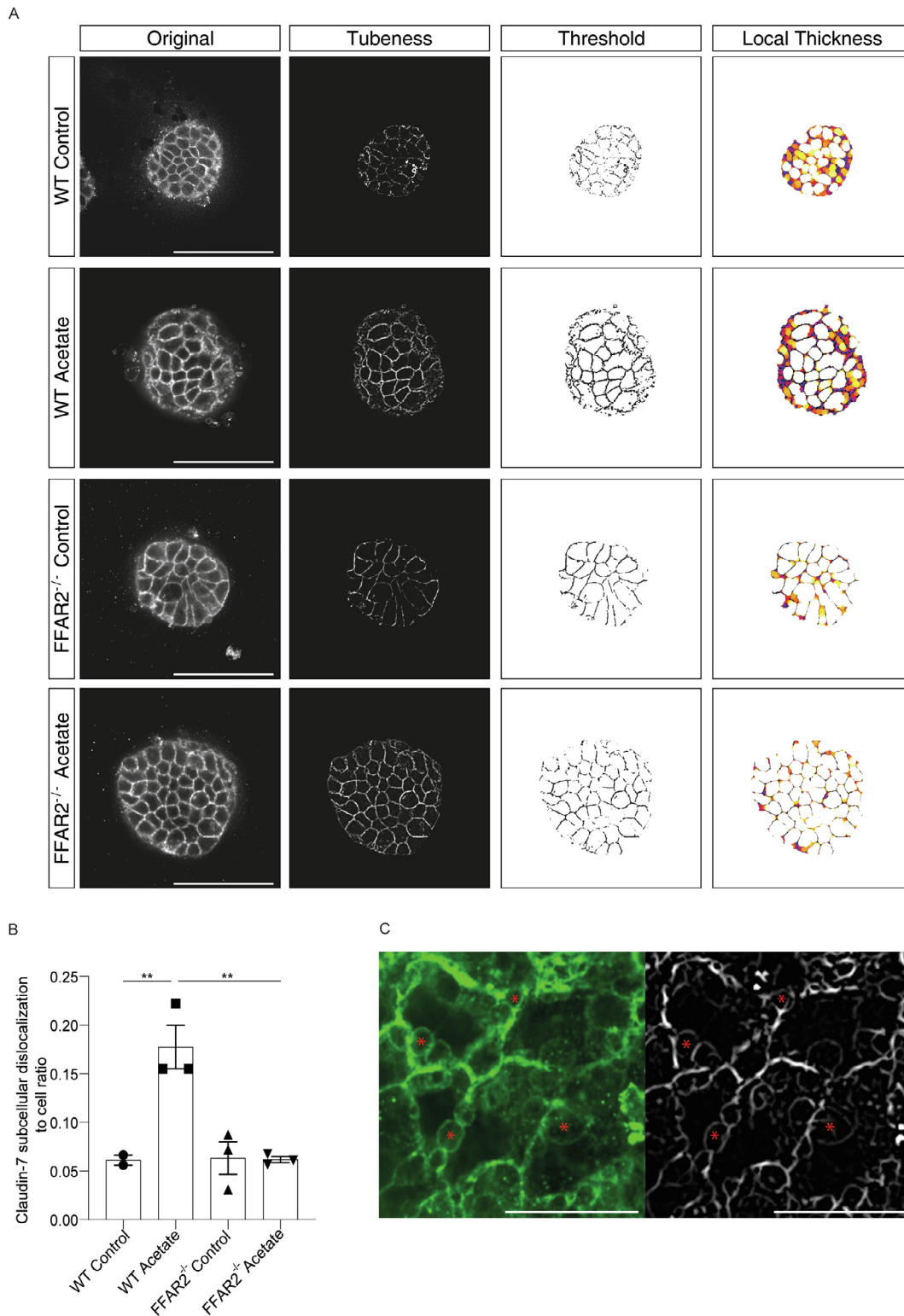
Fig. 4. Acetate treatment disorganizes Claudin-7 localization in murine intestinal organoids. (A) Wildtype and free fatty acid receptor 2 knockout (FFAR2$^{-/-}$) organoids after 24 h of acetate treatment (10 mM) stained for tight junction protein claudin-7. Original confocal images were processed using the FIJI tubeness filter plugin and afterwards local thickness was quantified using FIJI software. Darker colors mark small areas, e.g. areas of claudin-7 subcellular dislocalization, white color marks the biggest areas, e.g. cells. Treatment with PBS serves as a control (scale bars: 50 μm). (B) Quantification of local thickness analysis shows the number of pixels that fall under the threshold divided by the number of pixels that fall above the threshold (n = 3). Values were compared using one-way ANOVA. **$P < 0.01$. (C) Representative picture of claudin-7 staining (left) and a tubeness filtered image in an acetate-treated wildtype organoid. Asterisks indicate areas of claudin-7 subcellular dislocalization (scale bars = 10 μm).

It was shown that ESPs from *Haemonchus contortus, Teladorsagia circumsincta* and *Trichuris suis* increase intestinal epithelial permeability (Hiemstra et al., 2014; Rehman et al., 2016) and we confirmed these observations for HESPs. Even minor changes in paracellular permeability were shown to allow the diffusion of immunomodulatory ESPs through the epithelial barrier and modu-

lation of lamina propria dendritic cell (DC) function, and pro-inflammatory cytokine secretion (Massacand et al., 2009; Hiemstra et al., 2014). Therefore, acetate-mediated increased para-cellular permeability would allow *H. polygyrus* L3s to prime lamina propria lymphocyte function behind the epithelial barrier prior to their actual epithelial penetration. Knowing the crucial role of epithelial cell-derived alarmins such as IL-25, IL-33 and thymic stromal lymphopoietin (TSLP), and reports showing that helminth ESP modulates their secretion (Hiemstra et al., 2014), it would represent an additional beneficial mechanism to target the lamina propria lymphocytes directly. However, the exact ESP-derived effector molecule responsible for this effect on barrier permeability remains unknown (Faniyi et al., 2020). Here we identified the SCFA acetate – that was shown to be also secreted by other helminths (Tielens et al., 2010) – as one key effector molecule promoting intestinal epithelial permeability via FFAR2 binding on IEC. This effect could be partly mediated through delocalization of the TJ protein claudin-7. We focused on claudin-7 as there had been major differences observed following acetate treatment and it was shown that epithelial claudin-7 knockout leads to an imbalance in the paracellular flux of intestinal small organic solutes, promotes the degradation of intestinal extracellular matrix and induces intestinal inflammation (Tanaka et al., 2015). Claudin-7 is highly expressed in IECs of mice (Fujita et al., 2006) and was shown to be essential for steady state barrier function (Lioni et al., 2007; Wang et al., 2018; Xing et al., 2020). Its dysregulation or disorganisation leads to lowered E-cadherin expression as well as lowered cell–cell adhesion (Lioni et al., 2007). Su et al. (2011) also showed that infection with *H. polygyrus* changes colonic epithelial TJ morphologies. Similar changes are also seen in the intestinal organoid claudin-7 staining in the current study.

We previously showed that intestinal acetate concentrations are significantly increased during later stages of helminth infection (Zaiss et al., 2015). This is due to the acetate production by helminths but also due to the altered host intestinal microbiota composition (Zaiss et al., 2015). These results suggest that acetate is also beneficial to helminths during the chronic phase of infection. It has been shown that *H. polygyrus* has the ability to change the host immune response (Massacand et al., 2009; Grainger et al., 2010; Mosconi et al., 2015) and that this is at least partially mediated by SCFA binding to free fatty acid receptors (Zaiss et al., 2015). However, the permeability increasing effect of acetate shown in this study might contribute to this as well.

There are reports about the proven beneficial effect on inflammatory bowel disease (IBD) – an impaired intestinal barrier disease - following helminth infections (Hunter and McKay, 2004; Sipahi and Baptista, 2017; Maruszewska-Cheruiyot et al., 2018) which, at first glance, are obviously contradictory to our finding. However, the amelioration of IBD by helminths is based on the induction of protective adaptive immune responses such as regulatory T-cells following infection (Finney et al., 2007; Setiawan et al., 2007) and independent of our results observed here, have an initial and locally limited effect on IEC permeability.

Interestingly, Feng et al. (2018) recently showed in Caco-2 cell line monolayers that besides the well-known barrier protective effects of the SCFA butyrate (Peng et al., 2007, 2009; Parada Venegas et al., 2019b), acetate alone or in combination with butyrate increased transepithelial resistance as measured by a standard Millicell-ERS voltohmmeter. A combination of SCFA (acetate, propionate and butyrate) was shown to prevent LPS-induced barrier dysfunction (Feng et al., 2018). However, in our hands only acetate increased barrier permeability as opposed to just propionate and butyrate – most likely through previously described effects of butyrate on histone deacetylases (HDAC) activity (Davie, 2003; Steliou et al., 2012; Chriett et al., 2019). Acetate treatment alone further enhanced epithelial permeability assessed using the fully automatic live Maestro Z system. Our observations were further confirmed by functionally and physiologically relevant ex vivo organoid experiments where acetate effects could be rescued by a lack of FFAR2 expression in IECs. The discrepancies observed in Caco-2 experiments between the two studies may be explained by different experimental settings, such as timing and duration of acetate treatment or the level of confluence of Caco-2 cells.

What remains to be addressed in future is the question about the actual source of acetate during *H. polygyrus* infection. We showed in our previous publication that mature *H. polygyrus* L5s secrete detectable amounts of acetate in the ex vivo culture supernatants (Zaiss et al., 2015) In this ex vivo *H. polygyrus* L5 culture, antibiotics are added to maintain the culture sterility for up to 14 days and any bacterial contamination can be excluded. That strongly suggests that the detected ex vivo *H. polygyrus* L5 culture acetate levels were *H. polygyrus*-derived. However, at the same time intestinal content acetate levels were below the detection limit in antibiotic-treated mice over 4 weeks, highlighting the essential requirement for the microbiota to ferment fiber-rich diets into SCFAs such as acetate (Zaiss et al., 2015). Together with our here presented findings that in supernatants form ex vivo *H. polygyrus* L3s acetate levels can be detected, we must conclude that vast majority of acetate found in serum derives from the microbiota and the in vivo *H. polygyrus*-secreted acetate can only locally influence the surrounding tissue microenvironment. However, it would be wrong to separate these two findings, as they are somehow interconnected. If we look at acetate concentrations in sera and intestinal contents over time in *H. polygyrus*-infected mice, we see a 2–3-fold increase over the naïve setting (Zaiss et al., 2015). As we also clearly showed that *H. polygyrus* changes the microbiota composition (Rapin et al., 2020), it must be a combination of both *H. polygyrus* and microbiota-derived acetate. At this time, we can only speculate that *H. polygyrus*-sourced acetate might be one mechanism in the process of the microbiota being modulated in favor of more microbiota-derived acetate. It was shown that acetate could be taken up from particular bacteria as an energy source, thereby providing a competitive advantage that allows microbial changes.

In conclusion, our study unravels a new mechanism for helminth-derived SCFA acetate in modulating intestinal barrier function. Future studies need to address the downstream signaling following acetate FFAR2 activation and its direct effects on TJ delocalization and assembly. Mucin-inducing properties of acetate (Takeuchi et al., 2021), as well as modulations of the microbiota composition, in addition to its effects on the paracellular permeability, should also be considered in future studies. As a final note, the mechanisms involved in alcohol abuse leading to disruption of intestinal barrier integrity and increasing permeability is not yet completely understood (Calleja-Conde et al., 2021). Excessive alcohol consumption was shown to increase acetate concentrations, the primary metabolic end product of ethanol (Azizov et al., 2020), and could thereby impact intestinal barrier function as a matter for speculation. At the same time, moderate ethanol consumption together with systemically increased acetate concentrations were reported to have anti-inflammatory effects (Azizov and Zaiss, 2021) by modulating proper local T follicular helper cell functions (Azizov et al., 2020). Taken together, these results underline the idea of a spatial- and concentration-dependent effect of acetate.

Appendix A. Supplementary data

Supplementary data to this article can be found online at https://doi.org/10.1016/j.ijpara.2022.04.004.

References

Angelow, S., Ahlstrom, R., Yu, A.S., 2008. Biology of claudins. Am. J. Physiol. Renal Physiol. 295, F867–F876.

Anthony, R.M., Rutitzky, L.I., Urban Jr., J.F., Stadecker, M.J., Gause, W.C., 2007. Protective immune mechanisms in helminth infection. Nat. Rev. Immunol. 7, 975–987.

Azizov, V., Dietel, K., Steffen, F., Dürholz, K., Meidenbauer, J., Lucas, S., Frech, M., Omata, Y., Tajik, N., Knipfer, L., Kolenbrander, A., Seubert, S., Lapuente, D., Sokolova, M.V., Hofmann, J., Tenbusch, M., Ramming, A., Steffen, U., Nimmerjahn, F., Linker, R., Wirtz, S., Herrmann, M., Temchura, V., Sarter, K., Schett, G., Zaiss, M.M., 2020. Ethanol consumption inhibits TFH cell responses and the development of autoimmune arthritis. Nat. Commun. 11, 1998.

Azizov, V., Zaiss, M.M., 2021. Alcohol consumption in rheumatoid arthritis: A path through the immune system. Nutrients 13, 1324.

Bardenbacher, M., Ruder, B., Britzen-Laurent, N., Schmid, B., Waldner, M., Naschberger, E., Scharl, M., Muller, W., Gunther, C., Becker, C., Sturzl, M., Tripal, P., 2019. Permeability analyses and three dimensional imaging of interferon gamma-induced barrier disintegration in intestinal organoids. Stem Cell Res. 35, 101383.

Behnke, J.M., Menge, D.M., Noyes, H., 2009. *Heligmosomoides bakeri*: a model for exploring the biology and genetics of resistance to chronic gastrointestinal nematode infections. Parasitology 136, 1565–1580.

Benson, K., Cramer, S., Galla, H.J., 2013. Impedance-based cell monitoring: barrier properties and beyond. Fluids Barriers CNS 10, 5.

Brown, A.J., Goldsworthy, S.M., Barnes, A.A., Eilert, M.M., Tcheang, L., Daniels, D., Muir, A.I., Wigglesworth, M.J., Kinghorn, I., Fraser, N.J., Pike, N.B., Strum, J.C., Steplewski, K.M., Murdock, P.R., Holder, J.C., Marshall, F.H., Szekeres, P.G., Wilson, S., Ignar, D.M., Foord, S.M., Wise, A., Dowell, S.J., 2003. The orphan G protein-coupled receptors GPR41 and GPR43 are activated by propionate and other short chain carboxylic acids. J. Biol. Chem. 278, 11312–11319.

Brown, A.J., Jupe, S., Briscoe, C.P., 2005. A family of fatty acid binding receptors. DNA Cell Biol. 24, 54–61.

Calleja-Conde, J., Echeverry-Alzate, V., Bühler, K.-M., Durán-González, P., Morales-García, J.Á., Segovia-Rodríguez, L., Rodríguez de Fonseca, F., Giné, E., López-Moreno, J.A., 2021. The immune system through the lens of alcohol intake and gut microbiota. Int. J. Mol. Sci. 22, 7485.

Chriett, S., Dabek, A., Wojtala, M., Vidal, H., Balcerczyk, A., Pirola, L., 2019. Prominent action of butyrate over beta-hydroxybutyrate as histone deacetylase inhibitor, transcriptional modulator and anti-inflammatory molecule. Sci. Rep. 9, 742.

D'Souza, W.N., Douangpanya, J., Mu, S., Jaeckel, P., Zhang, M., Maxwell, J.R., Rottman, J.B., Labitzke, K., Willee, A., Beckmann, H., Wang, Y., Li, Y., Schwandner, R., Johnston, J.A., Towne, J.E., Hsu, H., 2017. Differing roles for short chain fatty acids and GPR43 agonism in the regulation of intestinal barrier function and immune responses. PLoS ONE 12, e0180190.

Daïen, C.I., Tan, J., Audo, R., Mielle, J., Quek, L.E., Krycer, J.R., Angelatos, A., Duraes, M., Pinget, G., Ni, D., Robert, R., Alam, M.J., Amian, M.C.B., Sierro, F., Parmar, A., Perkins, G., Hoque, S., Gosby, A.K., Simpson, S.J., Ribeiro, R.V., Mackay, C.R., Macia, L., 2021. Gut-derived acetate promotes B10 cells with antiinflammatory effects. JCI Insight 6 (7), e144156.

Davie, J.R., 2003. Inhibition of histone deacetylase activity by butyrate. J. Nutr. 133, 2485S–2493S.

de Silva, N.R., Brooker, S., Hotez, P.J., Montresor, A., Engels, D., Savioli, L., 2003. Soil-transmitted helminth infections: updating the global picture. Trends Parasitol. 19, 547–551.

den Besten, G., van Eunen, K., Groen, A.K., Venema, K., Reijngoud, D.J., Bakker, B.M., 2013. The role of short-chain fatty acids in the interplay between diet, gut microbiota, and host energy metabolism. J. Lipid Res. 54, 2325–2340.

Elamin, E.E., Masclee, A.A., Dekker, J., Pieters, H.J., Jonkers, D.M., 2013. Short-chain fatty acids activate AMP-activated protein kinase and ameliorate ethanol-induced intestinal barrier dysfunction in Caco-2 cell monolayers. J. Nutr. 143, 1872–1881.

Faniyi, A.A., Wijanarko, K.J., Tollitt, J., Worthington, J.J., 2020. Helminth sensing at the intestinal epithelial barrier-a taste of things to come. Front. Immunol. 11, 1489.

Fasano, A., 2012. Zonulin, regulation of tight junctions, and autoimmune diseases. Ann. N. Y. Acad. Sci. 1258, 25–33.

Feng, Y.H., Wang, Y., Wang, P., Huang, Y.L., Wang, F.J., 2018. Short-chain fatty acids manifest stimulative and protective effects on intestinal barrier function through the inhibition of NLRP3 inflammasome and autophagy. Cell. Physiol. Biochem. 49, 190–205.

Finney, C.A., Taylor, M.D., Wilson, M.S., Maizels, R.M., 2007. Expansion and activation of CD4(+)CD25(+) regulatory T cells in *Heligmosomoides polygyrus* infection. Eur. J. Immunol. 37, 1874–1886.

Fujita, H., Chiba, H., Yokozaki, H., Sakai, N., Sugimoto, K., Wada, T., Kojima, T., Yamashita, T., Sawada, N., 2006. Differential expression and subcellular localization of claudin-7, -8, -12, -13, and -15 along the mouse intestine. J. Histochem. Cytochem. 54, 933–944.

Grainger, J.R., Smith, K.A., Hewitson, J.P., McSorley, H.J., Harcus, Y., Filbey, K.J., Finney, C.A.M., Greenwood, E.J.D., Knox, D.P., Wilson, M.S., Belkaid, Y., Rudensky, A.Y., Maizels, R.M., 2010. Helminth secretions induce de novo T cell Foxp3 expression and regulatory function through the TGF-β pathway. J. Exp. Med. 207, 2331–2341.

Harris, N., Gause, W.C., 2011. To B or not to B: B cells and the Th2-type immune response to helminths. Trends Immunol. 32, 80–88.

Harris, N.L., Pleass, R., Behnke, J.M., 2014. Understanding the role of antibodies in murine infections with *Heligmosomoides (polygyrus) bakeri*: 35 years ago, now and 35 years ahead. Parasite Immunol. 36, 115–124.

Hiemstra, I.H., Klaver, E.J., Vrijland, K., Kringel, H., Andreasen, A., Bouma, G., Kraal, G., van Die, I., den Haan, J.M., 2014. Excreted/secreted *Trichuris suis* products reduce barrier function and suppress inflammatory cytokine production of intestinal epithelial cells. Mol. Immunol. 60, 1–7.

Hunter, M.M., McKay, D.M., 2004. Review article: helminths as therapeutic agents for inflammatory bowel disease. Aliment. Pharmacol. Ther. 19, 167–177.

Johnston, C.J.C., Robertson, E., Harcus, Y., Grainger, J.R., Coakley, G., Smyth, D.J., McSorley, H.J., Maizels, R., 2015. Cultivation of *Heligmosomoides polygyrus*: an immunomodulatory nematode parasite and its secreted products. J. Vis. Exp. 98. e52412–e52412.

Kim, C.H., 2021. Control of lymphocyte functions by gut microbiota-derived short-chain fatty acids. Cell. Mol. Immunol. 18, 1161–1171.

Landy, J., Ronde, E., English, N., Clark, S.K., Hart, A.L., Knight, S.C., Ciclitira, P.J., Al-Hassi, H.O., 2016. Tight junctions in inflammatory bowel diseases and inflammatory bowel disease associated colorectal cancer. World J. Gastroenterol. 22, 3117–3126.

Le Poul, E., Loison C., S., Struyf S., Springael J.-Y., Lannoy, V., Decobecq M.-E., Brezillon S., Dupriez V., Vassart G., Van Damme, J., Parmentier, M., Detheux, M., 2003. Functional characterization of human receptors for short chain fatty acids and their role in polymorphonuclear cell activation. 278, 25481–25489.

Lioni, M., Brafford, P., Andl, C., Rustgi, A., El-Deiry, W., Herlyn, M., Smalley, K.S.M., 2007. Dysregulation of claudin-7 leads to loss of E-cadherin expression and the increased invasion of esophageal squamous cell carcinoma cells. Am. J. Pathol. 170, 709–721.

Lloyd, C.-A.-O., Snelgrove, R.-A.-O., 2018. Type 2 immunity: Expanding our view. Sci. Immunol. 3 (25).

Lu, Z., Ding, L., Lu, Q., Chen, Y.H., 2013. Claudins in intestines: Distribution and functional significance in health and diseases. Tissue Barriers 1, e24978.

Lucas, S., Omata, Y., Hofmann, J., Bottcher, M., Iljazovic, A., Sarter, K., Albrecht, O., Schulz, O., Krishnacoumar, B., Kronke, G., Herrmann, M., Mougiakakos, D., Strowig, T., Schett, G., Zaiss, M.M., 2018. Short-chain fatty acids regulate systemic bone mass and protect from pathological bone loss. Nat. Commun. 9, 55.

Maruszewska-Cheruiyot, M., Donskow-Lysoniewska, K., Doligalska, M., 2018. Helminth therapy: advances in the use of parasitic worms against inflammatory bowel diseases and their challenges. Helminthologia 55, 1–11.

Massacand, J.C., Stettler, R.C., Meier, R., Humphreys, N.E., Grencis, R.K., Marsland, B. J., Harris, N.L., 2009. Helminth products bypass the need for TSLP in Th2 immune responses by directly modulating dendritic cell function. Proc. Natl. Acad. Sci. U. S. A. 106, 13968–13973.

McKay, D.M., Shute, A., Lopes, F., 2017. Helminths and intestinal barrier function. Tissue Barriers 5, e1283385.

Mosconi, I., Dubey, L.K., Volpe, B., Esser-von Bieren, J., Zaiss, M.M., Lebon, L., Massacand, J.C., Harris, N.L., 2015. Parasite proximity drives the expansion of regulatory T cells in peyer's patches following intestinal helminth infection. Infect. Immun. 83, 3657–3665.

Moyat, M., Coakley, G., Harris, N.L., 2019. The interplay of type 2 immunity, helminth infection and the microbiota in regulating metabolism. Clin. Transl. Immunol. 8, e01089.

Nilsson, N.E., Kotarsky, K., Owman, C., Olde, B., 2003. Identification of a free fatty acid receptor, FFA2R, expressed on leukocytes and activated by short-chain fatty acids. Biochem. Biophys. Res. Commun. 303, 1047–1052.

Ohata, A., Usami, M., Miyoshi, M., 2005. Short-chain fatty acids alter tight junction permeability in intestinal monolayer cells via lipoxygenase activation. Nutrition 21, 838–847.

Parada Venegas, D., De la Fuente, M.K., Landskron, G., Gonzalez, M.J., Quera, R., Dijkstra, G., Harmsen, H.J.M., Faber, K.N., Hermoso, M.A., 2019a. Short chain fatty acids (SCFAs)-mediated gut epithelial and immune regulation and its relevance for inflammatory bowel diseases. Front. Immunol. 10, 277.

Parada Venegas, D., De la Fuente, M.K., Landskron, G., González, M.J., Quera, R., Dijkstra, G., Harmsen, H.J.M., Faber, K.N., Hermoso, M.A., 2019b. Short chain fatty acids (SCFAs)-mediated gut epithelial and immune regulation and its relevance for inflammatory bowel diseases. Front. Immunol. 10, 277.

Peng, L., He, Z., Chen, W., Holzman, I.R., Lin, J., 2007. Effects of butyrate on intestinal barrier function in a Caco-2 cell monolayer model of intestinal barrier. Pediatr. Res. 61, 37–41.

Peng, L., Li, Z.R., Green, R.S., Holzman, I.R., Lin, J., 2009. Butyrate enhances the intestinal barrier by facilitating tight junction assembly via activation of AMP-activated protein kinase in Caco-2 cell monolayers. J. Nutr. 139, 1619–1625.

Qiu, J., Villa, M., Sanin, D.E., Buck, M.D., O'Sullivan, D., Ching, R., Matsushita, M., Grzes, K.M., Winkler, F., Chang, C.H., Curtis, J.D., Kyle, R.L., Van Teijlingen Bakker, N., Corrado, M., Haessler, F., Alfei, F., Edwards-Hicks, J., Maggi Jr., L.B., Zehn, D., Egawa, T., Bengsch, B., Klein Geltink, R.I., Jenuwein, T., Pearce, E.J., Pearce, E.L., 2019. Acetate promotes T Cell effector function during glucose restriction. Cell Rep. 27. 2063–2074 e2065.

Rapin, A., Chuat, A., Lebon, L., Zaiss, M.M., Marsland, B.J., Harris, N.L., 2020. Infection with a small intestinal helminth, *Heligmosomoides polygyrus bakeri*, consistently alters microbial communities throughout the murine small and large intestine. Int. J. Parasitol. 50, 35–46.

Rehman, Z.U., Deng, Q., Umair, S., Savoian, M.S., Knight, J.S., Pernthaner, A., Simpson, H.V., 2016. Excretory/secretory products of adult *Haemonchus contortus* and *Teladorsagia circumcincta* which increase the permeability of Caco-2 cell monolayers are neutralised by antibodies from immune hosts. Vet. Parasitol. 221, 104–110.

Reynolds, L.A., Filbey, K.J., Maizels, R.M., 2012. Immunity to the model intestinal helminth parasite *Heligmosomoides polygyrus*. Semin. Immunopathol. 34, 829–846.

Sato, T., Vries, R.G., Snippert, H.J., van de Wetering, M., Barker, N., Stange, D.E., van Es, J.H., Abo, A., Kujala, P., Peters, P.J., Clevers, H., 2009. Single Lgr5 stem cells build crypt-villus structures in vitro without a mesenchymal niche. Nature 459, 262–265.

Setiawan, T., Metwali, A., Blum, A.M., Ince, M.N., Urban Jr., J.F., Elliott, D.E., Weinstock, J.V., 2007. *Heligmosomoides polygyrus* promotes regulatory T-cell cytokine production in the murine normal distal intestine. Infect. Immun. 75, 4655–4663.

Sina, C., Gavrilova O., Förster, M., Till, A., Derer, S., Hildebrand, F., Raabe, B., Chalaris, A., Scheller, J., Rehmann, A., Franke, A., Ott, S., Häsler, R., Nikolaus, S., Fölsch, U.R., Rose-John, S., Jiang, H.-P., Li, J., Schreiber, S., Rosenstiel, P., 2009. G protein-coupled receptor 43 is essential for neutrophil recruitment during intestinal inflammation. J. Immunol. 183, 7514–7522.

Sipahi, A.M., Baptista, D.M., 2017. Helminths as an alternative therapy for intestinal diseases. World J. Gastroenterol. 23, 6009–6015.

Sivaprakasam, S., Prasad, P.D., Singh, N., 2016. Benefits of short-chain fatty acids and their receptors in inflammation and carcinogenesis. Pharmacol. Ther. 164, 144–151.

Steliou, K., Boosalis, M.S., Perrine, S.P., Sangerman, J., Faller, D.V., 2012. Butyrate histone deacetylase inhibitors. Biores. Open Access 1, 192–198.

Su, C.W., Cao, Y., Kaplan, J., Zhang, M., Li, W., Conroy, M., Walker, W.A., Shi, H.N., 2011. Duodenal helminth infection alters barrier function of the colonic epithelium via adaptive immune activation. Infect. Immun. 79, 2285–2294.

Sutton, T.L., Zhao, A., Madden, K.B., Elfrey, J.E., Tuft, B.A., Sullivan, C.A., Urban Jr., J.F., Shea-Donohue, T., 2008. Anti-Inflammatory mechanisms of enteric *Heligmosomoides polygyrus* infection against trinitrobenzene sulfonic acid-induced colitis in a murine model. Infect. Immun. 76, 4772–4782.

Tajik, N., Frech, M., Schulz, O., Schalter, F., Lucas, S., Azizov, V., Durholz, K., Steffen, F., Omata, Y., Rings, A., Bertog, M., Rizzo, A., Iljazovic, A., Basic, M., Kleyer, A., Culemann, S., Kronke, G., Luo, Y., Uberla, K., Gaipl, U.S., Frey, B., Strowig, T., Sarter, K., Bischoff, S.C., Wirtz, S., Canete, J.D., Ciccia, F., Schett, G., Zaiss, M.M., 2020. Targeting zonulin and intestinal epithelial barrier function to prevent onset of arthritis. Nat. Commun. 11, 1995.

Takeuchi, T., Miyauchi, E., Kanaya, T., Kato, T., Nakanishi, Y., Watanabe, T., Kitami, T., Taida, T., Sasaki, T., Negishi, H., Shimamoto, S., Matsuyama, A., Kimura, I., Williams, I.R., Ohara, O., Ohno, H., 2021. Acetate differentially regulates IgA reactivity to commensal bacteria. Nature 595, 560–564.

Tanaka, H., Takechi, M., Kiyonari, H., Shioi, G., Tamura, A., Tsukita, S., 2015. Intestinal deletion of Claudin-7 enhances paracellular organic solute flux and initiates colonic inflammation in mice. Gut 64, 1529–1538.

Thorburn, A.N., McKenzie, C.I., Shen, S., Stanley, D., Macia, L., Mason, L.J., Roberts, L.K., Wong, C.H., Shim, R., Robert, R., Chevalier, N., Tan, J.K., Marino, E., Moore, R.J., Wong, L., McConville, M.J., Tull, D.L., Wood, L.G., Murphy, V.E., Mattes, J., Gibson, P.G., Mackay, C.R., 2015. Evidence that asthma is a developmental origin disease influenced by maternal diet and bacterial metabolites. Nat. Commun. 6, 7320.

Tielens, A.G., van Grinsven, K.W., Henze, K., van Hellemond, J.J., Martin, W., 2010. Acetate formation in the energy metabolism of parasitic helminths and protists. Int. J. Parasitol. 40, 387–397.

Wang, M.P.J., Johnston, C.J.C., Grainger, J.R., Konkel, J.E., O'Connor, R.A., Anderton, S. M., Maizels, R.M., 2020. The helminth parasite *Heligmosomoides polygyrus* attenuates EAE in an IL-4Ralpha-dependent manner. Front. Immunol. 11, 1830.

Wojciechowski, W., Harris, D.P., Sprague, F., Mousseau, B., Makris, M., Kusser, K., Honjo, T., Mohrs, K., Mohrs, M., Randall, T., Lund, F.E., 2009. Cytokine-producing effector B cells regulate type 2 immunity to *H. polygyrus*. Immunity 30, 421–433.

Wolff, M.J., Broadhurst, M.J., Loke, P., 2012. Helminthic therapy: improving mucosal barrier function. Trends Parasitol. 28, 187–194.

Xing, T., Benderman, L.J., Sabu, S., Parker, J., Yang, J., Lu, Q., Ding, L., Chen, Y.H., 2020. Tight junction protein claudin-7 is essential for intestinal epithelial stem cell self-renewal and differentiation. Cell Mol. Gastroenterol. Hepatol. 9, 641–659.

Yap, Y.A., McLeod, K.H., McKenzie, C.I., Gavin, P.G., Davalos-Salas, M., Richards, J.L., Moore, R.J., Lockett, T.J., Clarke, J.M., Eng, V.V., Pearson, J.S., Hamilton-Williams, E.E., Mackay, C.R., Marino, E., 2021. An acetate-yielding diet imprints an immune and anti-microbial programme against enteric infection. Clin. Transl. Immunol. 10, e1233.

Zaiss, M.M., Rapin, A., Lebon, L., Dubey, L.K., Mosconi, I., Sarter, K., Piersigilli, A., Menin, L., Walker, A.W., Rougemont, J., Paerewijck, O., Geldhof, P., McCoy, K.D., Macpherson, A.J., Croese, J., Giacomin, P.R., Loukas, A., Junt, T., Marsland, B.J., Harris, N.L., 2015. The intestinal microbiota contributes to the ability of helminths to modulate allergic inflammation. Immunity 43, 998–1010.